NASA Contractor Report 198319

ICASE Report No. 96-24

ICASE

KOLMOGOROV FLOW IN THREE DIMENSIONS

John V. Shebalin
Stephen L. Woodruff

NASA Contract No. NAS1-19480
March 1996

Institute for Computer Applications in Science and Engineering
NASA Langley Research Center
Hampton, VA 23681-0001

Operated by Universities Space Research Association

National Aeronautics and
Space Administration

Langley Research Center
Hampton, Virginia 23681-0001

Kolmogorov Flow in Three Dimensions

John V. Shebalin

Aerodynamic and Acoustic Methods Branch

Langley Research Center, National Aeronautics and Space Administration, Hampton, Virginia 23681

Stephen L. Woodruff[a]

Institute for Computer Applications in Science and Engineering

Langley Research Center, National Aeronautics and Space Administration, Hampton, Virginia 23681

ABSTRACT

A numerical study of the long-time evolution of incompressible Navier-Stokes turbulence forced at a single long-wavelength Fourier mode, *i.e.*, a Kolmogorov flow, has been completed. The boundary conditions are periodic in three dimensions and the forcing is effected by imposing a steady, two-dimensional, sinusoidal shear velocity which is directed along the x-direction and varies along the z-direction. A comparison with experimental data shows agreement with measured cross-correlations of the turbulent velocity components which lie in the mean-flow plane. A statistical analysis reveals that the shear-driven turbulence studied here has significant spectral anisotropy which increases with wave number.

[a]This research was supported by the National Aeronautics and Space Administraton under NASA Contract No. NAS1-19480 while the second author was in residence at the Institute for Computer Applications in Science and Engineering (ICASE), NASA Langley Research Center, Hampton, VA 23681-0001.

I. Introduction

The presence of an unstable mean shear (*i.e.*, a nonzero time-averaged velocity gradient) is the essential source of turbulent fluctuations in any given fluid dynamical system. The mean shear is maintained by suitable external forces and, if the system contains a region of fully developed turbulent flow which exists long enough for study, then meaningful statistical statements can be made concerning it. For example, the characteristics of statistically stationary flow through pipes and channels [1, 2, 3, 4] and over flat plates [5, 6] have been carefully observed experimentally for over a century.

While the laminar pipe flow profile is parabolic, an even simpler laminar profile is a linear one. Thus, in the last several decades there have been a number of physical experiments measuring the characteristics of incompressible fluid turbulence in the presence of a steady linear velocity gradient [7, 8, 9, 10] (with regard to the results of [8], however, see [11]). This basic flow has also been simulated numerically, although the numerical procedure is rather complicated, since difficulties arise in treating the turbulent flow as homogeneous, (*i.e.*, with periodic boundary conditions) while simultaneously imposing a non-periodic linear shear profile to drive the flow [12, 13, 14, 15].

Here, another basic flow is utilized to examine forced, dissipative turbulence: An erstwhile homogeneous flow forced by a *sinusoidal* shear profile. This steady sinusoidal shear has a wavelength equal to an edge-length of the periodic box, where the imposed velocity is always in the x-direction but varies along the z-direction. The resulting motion, which can be considered as homogeneous in each xy-plane, but not in the z-direction, is a *Kolmogorov flow*. In previous work, transition and turbulence of two-dimensional Kolmogorov flows have been discussed [16, 17, 18, 19, 20, 21, 22] and a study of three-dimensional Kolmogorov flow in the presence of hyperviscosity was reported [23]; here, three-dimensional Kolmogorov flow turbulence with normal viscosity is numerically simulated and examined.

Near the zeroes of the sinusoidal shear velocity the profile is approximately linear, while near the extrema of the imposed velocity the profile is approximately parabolic. Heuristically, the basic Kolmogorov flow can be thought of as a combination of a linear homogeneous shear profile and a laminar parabolic channel profile. As with these profiles (*i.e.*, Couette and Poiseuille flow [24]), an imposed sinusoidal shear velocity of sufficiently large amplitude is also unstable to perturbations [19]. Here, the amplitude is large enough so that instability occurs and turbulence results.

In brief, the purpose of this paper is to report on Fourier-method simulations of three-dimensional Kolmogorov turbulence. This will provide a numerical flow history with which comparisons to physical experiments can be made. This numerical record will then allow some aspects of physical and spectral anisotropy to be illustrated.

In the next section, the basic equations and qualitative features of their solution are presented. Following this, the numerical procedure is briefly discussed and numerical results are compared with pertinent experimental ones. Finally, a discussion and conclusions are given.

II. Basic Equations

In vorticity form, the equations which describe incompressible Navier-Stokes flow are

$$\partial_t \boldsymbol{\Omega} \;=\; \nabla \times (\mathbf{V} \times \boldsymbol{\Omega}) + \nu \nabla^2 \boldsymbol{\Omega} + \nabla \times \mathbf{f} \tag{1}$$

Here, the total fluid velocity is $\mathbf{V}$, the vorticity is $\boldsymbol{\Omega} = \nabla \times \mathbf{V}$, and $\mathbf{f}$ is the external forcing applied to the fluid; for incompressibility, we also have $\nabla \cdot \mathbf{V} = 0$. Equation (1) is non-dimensional, so that $\nu = R_e^{-1}$, where R_e is the Reynolds number; additionally, the density has been set to unity. If the fluid is driven by an imposed velocity field $\mathbf{V}_o$ (where $\nabla \cdot \mathbf{V}_o = 0$, with associated vorticity $\boldsymbol{\Omega}_o = \nabla \times \mathbf{V}_o$), the total velocity and the total associated vorticity can be written as

$$\mathbf{V} = \mathbf{V}_o + \mathbf{u} \qquad \text{and} \qquad \boldsymbol{\Omega} = \boldsymbol{\Omega}_o + \boldsymbol{\omega} \tag{2}$$

where $\mathbf{u}$ is the velocity (satisfying $\nabla \cdot \mathbf{u} = 0$) and $\boldsymbol{\omega} = \nabla \times \mathbf{u}$ is the vorticity which arise from perturbations to the Kolmogorov flow:

$$\mathbf{V}_o = \hat{\mathbf{x}} A \sin z, \qquad \text{and} \qquad \boldsymbol{\Omega}_o = \hat{\mathbf{y}} A \cos z \; . \tag{3}$$

(When needed, the unit vectors $\hat{\mathbf{x}}$, $\hat{\mathbf{y}}$, and $\hat{\mathbf{z}}$, in the x-, y-, and z-directions, respectively, will be used). Placing (2) and (3) into (1) yields the basic equation of this paper:

$$\partial_t \boldsymbol{\omega} \;=\; \nabla \times [(\mathbf{u} + \mathbf{V}_o) \times (\boldsymbol{\omega} + \boldsymbol{\Omega}_o)] + \nu \nabla^2 \boldsymbol{\omega}. \tag{4}$$

In order to produce (4), the external force in (1) is $\mathbf{f} = \hat{\mathbf{x}} \nu A \sin z$; also, using (3), note that $\nabla \times (\mathbf{V}_o \times \boldsymbol{\Omega}_o) = 0$.

III. Qualitative Analysis

The model physical space in which the forced, dissipative turbulent flow is to occur will be a three-dimensional cube on which periodic boundary conditions are imposed. A qualitative picture of solutions to (4) can then be gained by using a discrete Fourier transformation to approximate these partial differential equations by a much larger, but finite, set of coupled ordinary differential equations. To do this, we use

$$\mathbf{u}(\mathbf{x},t) = \sum_{|\mathbf{k}|<N/2} \mathbf{u}(\mathbf{k},t)e^{\imath\mathbf{k}\cdot\mathbf{x}} \quad \text{and} \quad \boldsymbol{\omega}(\mathbf{x},t) = \sum_{|\mathbf{k}|<N/2} \boldsymbol{\omega}(\mathbf{k},t)e^{\imath\mathbf{k}\cdot\mathbf{x}}. \tag{5}$$

Here, $\imath = \sqrt{-1}$, and the sum (and each similar sum appearing henceforth) is over all $\mathbf{k}$ such that $k = |\mathbf{k}| < \frac{1}{2}N$, *i.e.*, the Fourier series is 'isotropically truncated' to ensure no inherent spectral bias; N is the number of points in each of the three spatial dimensions. The flow field is thus represented by commensurate sets of values on discrete points in physical space and in Fourier space: $\mathbf{x} = (x_i, y_j, z_k) = \frac{2\pi}{N}(i,j,k)$, $i,j,k \in \{0,1,\cdots,N-1\}$, and $\mathbf{k} = (l,m,n)$, $l,m,n \in \{-\frac{1}{2}N+1,\cdots,-1,0,1,\cdots,\frac{1}{2}N\}$ with $k = \sqrt{l^2+m^2+n^2} < \frac{1}{2}N$. The velocity and vorticity coefficients are related by $\mathbf{u}(\mathbf{k}) = \imath k^{-2}\mathbf{k}\times\boldsymbol{\omega}(\mathbf{k})$ and $\boldsymbol{\omega}(\mathbf{k}) = \imath\mathbf{k}\times\mathbf{u}(\mathbf{k})$. Since the physical space velocity and vorticity fields $\mathbf{u}(\mathbf{x})$ and $\boldsymbol{\omega}(\mathbf{x})$ are real, their Fourier coefficients satisfy $\mathbf{u}(\mathbf{k}) = \mathbf{u}^*(-\mathbf{k})$ and $\boldsymbol{\omega}(\mathbf{k}) = \boldsymbol{\omega}^*(-\mathbf{k})$, where '*' signifies complex conjugation (and explicit time-dependence in the argument has been dropped for brevity).

Putting (4) and (5) together and using $\dot{\boldsymbol{\omega}}(\mathbf{k}) = d\boldsymbol{\omega}(\mathbf{k})/dt$ leads to

$$\dot{\boldsymbol{\omega}}(\mathbf{k}) \;=\; \imath\mathbf{k}\times\sum_{|\mathbf{p}|<N/2}[\mathbf{u}(\mathbf{p})+\mathbf{V}_o(\mathbf{p})]\times[\boldsymbol{\omega}(\mathbf{k}-\mathbf{p})+\boldsymbol{\Omega}_o(\mathbf{k}-\mathbf{p})] \;-\; \nu k^2\boldsymbol{\omega}(\mathbf{k}). \tag{6}$$

Here the Fourier coefficients associated with (3) are

$$\mathbf{V}_o(\pm\mathbf{k}) = \pm\imath\frac{A}{2}\delta(\hat{\mathbf{z}}\mp\mathbf{k})\hat{\mathbf{x}} \qquad \text{and} \qquad \boldsymbol{\Omega}_o(\pm\mathbf{k}) = -\frac{A}{2}\delta(\hat{\mathbf{z}}\mp\mathbf{k})\hat{\mathbf{y}} \tag{7}$$

where $\delta(\mathbf{p}) = 0$ if $\mathbf{p}\neq\mathbf{0}$ and $\delta(\mathbf{p}) = 1$ if $\mathbf{p} = \mathbf{0}$ [i.e., $\delta(\mathbf{p})$ is the Krönecker delta function].

A complete qualitative analysis requires determining the *critical points* of (6), *i.e.*, the zeros of the right-hand-side. Although a full discussion is beyond the scope of this work, one critical point of (6) occurs when all $\boldsymbol{\omega}(\mathbf{k}) = 0$, that is, at the origin of the phase space of the independent real and imaginary parts of the Fourier coefficients. If we linearize (6) about this point, we have

$$\dot{\boldsymbol{\omega}}(\mathbf{k}) \;=\; \mathsf{R}^+(\mathbf{k})\cdot\boldsymbol{\omega}(\mathbf{k}-\mathbf{z}) + \mathsf{R}^-(\mathbf{k})\cdot\boldsymbol{\omega}(\mathbf{k}+\mathbf{z}) - \nu k^2\boldsymbol{\omega}(\mathbf{k}). \tag{8}$$

The tensors $\mathsf{R}^{\pm}(\mathbf{k})$ are real quantities; their components are

$$\mathsf{R}^{\pm}_{\alpha\beta}(\mathbf{k}) \;=\; \frac{A}{2}\,\epsilon_{\alpha\gamma\rho}\,k_\gamma\left[\frac{(k_y\delta_{\rho\beta}\pm\delta_{\rho z}\delta_{\beta y})}{|\mathbf{k}\mp\hat{\mathbf{z}}|^2}\pm(\delta_{\rho y}\delta_{\beta z}-\delta_{\rho z}\delta_{\beta y})\right] \qquad (9)$$

Here, repeated indices are summed over and $\epsilon_{\alpha\gamma\rho}$ is the completely antisymmetric tensor with $\epsilon_{xyz}=1$.

The coupled set of equations (8) presents a complicated eigenvalue problem which must be addressed to fully understand the nature of the critical point at the origin of the phase space. This will not be done here; instead, consider the following two-dimensional system, which will illustrate some general features of (8):

$$\begin{aligned}\dot{p} &= Bq-\nu p\\ \dot{q} &= Cp-\nu q\end{aligned} \qquad (10)$$

The system matrix implicit on the right-hand-side has eigenvalues $\lambda_\pm = -\nu\pm\sqrt{BC}$, so that the two independent solutions to (10) have time dependence $\sim\exp(\lambda_\pm t)$. Assuming $BC\approx\pm A^2$ with $A>0$, there are three cases: First, let $BC=-A^2$; then the two-dimensional system point will merely spiral into the origin, so that $p,\ q\to 0$ as $t\to\infty$. Second, let $BC=A^2$ with $0<A\le\nu$; in this case, the system point will head directly to the origin without spiraling (unless $A=\nu$, in which event it moves to a point offset from the origin). In the third case, let $BC=A^2$ with $\nu<A$; here, in general, the system point will diverge away from the origin exponentially with time.

Relating this simplified system behavior to that of (8), it is clear that for A sufficiently small in (9), the phase point associated with (8) will return to the origin for any small perturbation so that the origin is a stable fixed point - an attractor. However, as A is increased, there will come a time at which the phase point diverges in at least one direction in phase space; the associated mode will continue to grow until the system behavior is no longer linear; energy now leaves the growing mode not by dissipation as with the other modes, but by nonlinear transfer to these other modes, where it is eventually dissipated. Increasing A even further leads to more modes acting as energy sources (and fewer as sinks). The neighborhood of the critical point at the origin thus gains a multidimensional saddle point structure. (This is essentially the transition to turbulence described by Landau & Lifshitz [25], and for two-dimensional Kolmogorov flow, it has been demonstrated by She [19]).

Suppose that A is sufficiently large so that $\mathbf{u}(\mathbf{k})=\mathbf{0}$ is an unstable equilibrium; then, small perturbations will grow exponentially for some $\mathbf{u}(\mathbf{k})$. As the flow develops, the $\mathbf{u}(\mathbf{k})$ will generally behave as a collection

of random variables, *i.e.*, $\mathbf{u}(\mathbf{k})$ will have two parts, a time-averaged part $\bar{\mathbf{u}}(\mathbf{k})$ and a fluctuating part $\mathbf{v}(\mathbf{k})$:

$$\mathbf{u}(\mathbf{k}) = \bar{\mathbf{u}}(\mathbf{k}) + \mathbf{v}(\mathbf{k}) \qquad \bar{\mathbf{u}}(\mathbf{k}) = \frac{1}{T}\int_0^T \mathbf{u}(\mathbf{k})\, dt \tag{11}$$

where $\mathbf{k} \cdot \mathbf{u}(\mathbf{k}) = \mathbf{k} \cdot \mathbf{v}(\mathbf{k}) = 0$ (and the vorticity associated with $\mathbf{v}(\mathbf{k})$ will be denoted $\mathbf{w}(\mathbf{k}) = i\mathbf{k} \times \mathbf{v}(\mathbf{k})$). In this case, $\bar{\mathbf{u}}(\mathbf{k})$ may be another critial point. (Note that in [23] the mean flow is defined as the instantaneous flow associated with the mode $\mathbf{u}(\mathbf{k}_f)$, where $\mathbf{k}_f = (0, 0, 1)$ here; this obviates a direct comparison of results). Alternatively, $\mathbf{u}(\mathbf{k})$ may not have a *simple attractor* (a fixed point), but may have a *limit cycle* (a closed path in phase space), or even a *strange attractor* (an open path which is confined to a subspace of phase space which is often of fractal dimension [26]).

One way to determine which possibility actually occurs is to proceed numerically. This has, in fact, already been done for two-dimensional Kolmogorov flow transition and turbulence [19] and for three-dimensional, hyperviscous Kolmogorov flow [23]. For sufficiently large Reynolds number ($R_e \equiv \nu^{-1} > 30$ in [19] and $R_e > 13$ in [23]), turbulence occurs; here $\nu^{-1} = 2000$ (although the microscale Reynolds number $R_\lambda \approx 30$). Thus, only the turbulent flow regime is examined here (although the nature of the attractor will not be considered in any further detail).

IV Results

The basic equations in Fourier space (6) were solved numerically using a pseudospectral method, with N in (5) equal to 64. To integrate (6) forward in time, the dissipative term was treated implicitly using a backward Euler scheme, while the nonlinear terms were handled using a 'third-order partially corrected Adams-Bashforth' method [27]. The Fourier coefficients of the nonlinear terms were determined by first transforming the various factors into physical space, then forming the point-by-point products, and finally transforming these products back into Fourier space [28].

The time-step was $\Delta t = .0025$. The initial turbulence spectrum was $|\mathbf{u}(\mathbf{k})| \sim k^2 \exp -k^2/4$, with the $\mathbf{u}(\mathbf{k})$ having random phase; the total initial turbulent energy was 0.0025. There was an initial transient period during which the value of A in (7) was increased to $A = 1.5$ (from $A = 0.1$), and the viscosity in (6) was decreased to $\nu = 0.0005$ (from $\nu = 0.001$). After a quasi-steady state appeared to become established, the values of all the Fourier coefficients $\mathbf{u}(\mathbf{k})$ were saved for all integer values of t from $t = 150$ to $t = 650$,

inclusive, for a total of 501 time slices upon which to perform statistical evaluation.

During the data collection time, $t = 150$ to $t = 650$, the parameter values were fixed at $A = 1.5$ and $\nu = 0.0005$. Denoting the volume average of any quantity Q by $< Q >$, the root-mean-square (rms) shear value can be defined as $S =< \Omega_o^2 >^{1/2}$; using (3) and $A = 1.5$, we have $S \approx 1$. Thus the time variable t used here is equivalent to the scaled time variable St used in [15].

In Figures 1 and 2, some of the global quantities for the simulation between $t = 150$ and $t = 650$ are shown. In Figure 1, the energy and the enstrophy are presented: the energy is defined as $E = \frac{1}{2} < v^2 >$ and the enstrophy as $\Omega = \frac{1}{2} < w^2 >$. Thus, the rms velocity fluctuation appears to be around 0.08 and the rms vorticity fluctuation appears to be around 0.22. In Figure 2, the following quantities are given: the average or rms wave number, $k_{avg} = \sqrt{\Omega/E} = (\int k^2 E(k)dk / \int E(k)dk)^{1/2}$; the dissipation wave number, $k_D = (2\Omega)^{1/4}\nu^{-1/2}$; the microscale Reynolds number, $R_\lambda = \sqrt{2E}/(\nu k_{avg}) = (k_D/k_{avg})^2$. Since $k_D < N/2 = 32$, the simulation is apparently well resolved. This is also borne out by the average energy spectrum shown in Figure 3, which is the average of the 501 individual energy spectra for each of the time slices between $t = 150$ and $t = 650$. The average energy spectrum is approximately exponential, especially in the smaller scales, with $E(k) \sim e^{-0.26k}$.

Mean Kolmogorov flow is strongly anisotropic since it is driven by the imposed velocity (3). The associated turbulence may also be anisotropic; a detailed examination can be conducted by considering the spectral anisotropy of the turbulence. Two measures of this are the 'Kolmogorov anisotropy' and another we will term the 'k^2-anisotropy'. The Kolmogorov anisotropy $K_{\alpha\beta}(k)$ $(\alpha, \beta \in \{x, y, z\})$ is defined as follows:

$$K_{\alpha\beta}(k) = \frac{S_{\alpha\beta}(k)}{S_{xx}(k) + S_{yy}(k) + S_{zz}(k)}, \qquad S_{\alpha\beta}(k) = \sum_{|\mathbf{k}|=k} v_\alpha(\mathbf{k}) v_\beta(\mathbf{k}) \tag{12}$$

while the k^2-anisotropy $C_\alpha(k)$ $(\alpha \in \{x, y, z\})$ is defined as:

$$C_\alpha(k) = \frac{D_\alpha(k)}{D_x(k) + D_y(k) + D_z(k)}, \qquad D_\alpha(k) = \sum_{|\mathbf{k}|=k} k_\alpha^2 |\mathbf{v}(\mathbf{k})|^2. \tag{13}$$

The Kolmogorov anisotropy measures the spectral distribution of turbulent energy amongst the different components of the velocity, and thus quantifies the behavior of spectral transfer between the velocity components as a function of increasing wave number. On the other hand, k^2-anisotropy measures the geometrical shape of the total spectral energy distribution, *i.e.*, to what extent it has spherical, spheroidal, or ellipsoidal symmetry.

In Figures 4, 5, and 6, the results of time-averaging from $t = 150$ to $t = 650$ are presented: In Figure 4, the diagonal components of $K_{\alpha\beta}(k)$ and in Figure 5, the off-diagonal components of $K_{\alpha\beta}(k)$ are presented; in Figure 6, the components of $C_\alpha(k)$ are given. It is clear that spectral anisotropy persists and, in fact, increases as k increases, for the diagonal components of $K_{\alpha\beta}(k)$ and for the components of $C_\alpha(k)$. (Isotropy occurs when these components are all equal to $\frac{1}{3}$.)

As already mentioned, a number of experimental results have appeared for the case of turbulence in the presence of a linear shear ($\mathbf{V}_o = z\hat{\mathbf{x}}$) [7, 8, 9, 10]. The sinusoidal shear (3) used here approximates a linear shear around the values $z = \pi$ and $z = 2\pi = 0 \bmod 2\pi$, so that there may be a basis for comparison. To effect a comparison, the following xy-plane-averaged cross-correlations $Q_{\alpha\beta}$ and stress anisotropy vector B_α, related to the Reynolds stress tensor, were averaged and symmetrized in physical space:

$$Q_{\alpha\beta}(z) = \frac{< v_\alpha v_\beta >_z}{\sqrt{< v_\alpha^2 >_z < v_\beta^2 >_z}}, \quad \alpha\beta \in \{xy, yz, zx\}; \qquad B_\alpha(z) = \frac{< v_\alpha^2 >_z}{E_z} - \frac{2}{3}, \quad \alpha \in \{x, y, z\}. \tag{14}$$

The brackets $< \cdots >_z$ indicate an average over all points in the xy-plane in physical space corresponding to each of the N values of z; $E_z = \frac{1}{2} < v^2 >_z$ is the kinetic energy in a given z-plane. These planar averages were taken for each of the 501 time slices between $t = 150$ and $t = 650$, and then averaged together. These time-averages were further averaged by *symmetrizing*:

$$\begin{aligned} \bar{Q}_{\alpha\beta}(z) &= \frac{1}{4}[Q_{\alpha\beta}(z) + Q_{\alpha\beta}(2\pi - z) - Q_{\alpha\beta}(\pi - z) - Q_{\alpha\beta}(\pi + z)] \\ \bar{B}_\alpha(z) &= \frac{1}{4}[B_\alpha(z) + B_\alpha(2\pi - z) + B_\alpha(\pi - z) + B_\alpha(\pi + z)] \end{aligned} \tag{15}$$

where it must be remembered that all flow variable are periodic in z (so that $z \to z \bmod 2\pi$).

The results of this symmetrization are shown in Figure 7 for $\bar{Q}_{zx}(z)$ and in Figures 8, 9, and 10 for $\bar{B}_\alpha(z)$. (Components $\bar{Q}_{xy}(z)$ and $\bar{Q}_{yz}(z)$ were essentially zero for all z, and will not be shown.) The value $|\bar{Q}_{zx}(z)| \approx 0.45$ at $z = 0$ and π correlates extremely well with the existing experimental results, which are summarized in Table 1 (which itself draws from another summary appearing in [33]). Although the $\bar{B}_\alpha(z)$ values do not match up very well, there is also a substantial variation amongst the various experimental values, as Table 1 again shows. A possible explanation for large difference between values of the $\bar{B}_\alpha(z)$ for the flow examined here (sinusoidal shear) and those derived from linear shear experiments may lie in the enhanced mixing of the sinusoidal shear, which tends to equalize the average magnitudes of v_x and v_z. Additionally, the close match of $\bar{Q}_{zx}$ may indicate a more universal measure of shear-driven turbulence than

the $\bar{B}_\alpha(z)$ can provide.

V Discussion

The results shown in Figures 4 and 6 do not appear consistent with the assumption of isotropy on which the Kolmogorov theory of turbulence, which predicts that the energy spectrum in the 'inertial range' ($k_f << k << k_D$) has the form $E(k) \sim k^{-5/3}$, is partly based [29]. However, another assumption in the Kolmogorov theory, that of homogeneity, is also not met here; the presence of sinusoidal forcing means that homogeneity can only be assumed to exist in two dimensions. Additionally, the relatively low Reynolds number and consequent lack of an inertial range here (and in any practical direct numerical simulation) indicates the absence of the very spectral regime for which homogeneity is a useful concept.

Nevertheless, it has also been argued [30] "that in uniform shear flow near equilibrium, local [physical] isotropy can never constitute a systematic approximation, even in the limit of infinite Reynolds number." This view is, in fact, borne out by physical experiments over a wide variety of Reynolds numbers [2, 5, 31], where the relative strengths of fluctuations in different coordinate direction are consistently anisotropic (as Table 1 shows). In spite of the anisotropy, the $k^{-5/3}$ spectrum is still seen [2], particularly in the streamwise fluctuations.

The Kolmogorov spectrum $E(k) \sim k^{-5/3}$, which is well established experimentally in many types of flows [32], may depend more on its dimensional consistency and the assumption of power-law behavior, than on other prior assumptions (such as isotropy at the small scales, i.e., at large values of wave number). Nevertheless, Figures 4 and 6 unequivocally show anisotropic spectral behavior with increasing wave number, while Figures 8, 9, and 10 slow only slight anisotropy in physical space due to the bias of these physical-space measures of anisotropy toward the relatively isotropic large scales. Whether or not the spectral anisotropy is maintained with increasing numerical resolution is an open question.

VI Conclusions

In this paper, the results of a numerical simulation of three-dimensional Kolmogorov flow were presented. This simulation was done on a 64^3 grid, and run for a relatively long period: $T_{tot} = 500$ (2×10^5 time steps

at $\Delta t = .0025$), after a period of initial transience had passed (as already mentioned, this time is equivalent to the rms-shear-scaled time of [15]). The forcing wave number was the lowest possible ($k_f = 1$), in contrast to that of some previous two-dimensional studies [19, 22], where $k_f = 8$ was used. The numerical simulation produced a flow history consisting of 501 sets of complete Fourier coefficients, each set effectively a time-slice of the dynamic evolution, for every whole value of simulation time between $t = 150$ and $t = 650$. In analyzing the flow history, it was evident that the flow was in a near-equilibrium state (although inherent fluctuations will always be present).

One interesting result of the simulation presented here concerned the (normalized) Reynolds stress tensor: The 'cross-correlation' $\bar{Q}_{zx} \approx 0.45$, in keeping with experimental linear shear results and providing some validation of the numerical simulation. However, the stress anisotropy vector components were more nearly equal than experimental linear shear results portrayed, though it is clear that the $\bar{B}_\alpha$ from different sources had a large amount of variation, particularly in comparison to the $\bar{Q}_{zx}$ (as Table I shows). This corroborates, to some extent, those turbulence modelling assumptions which presume that the $\bar{B}_\alpha$ are essentially equal in fully turbulent flows.

The second interesting result of the simulation was that the turbulent fluctuations in the long-wavelength Kolmogorov flow appeared to have significant spectral anisotropy which increased with wave number. This anisotropy presumably resulted from the presence of forcing, as unforced turbulence was seen to be essentially isotropic at all wave numbers [34]. The importance of this result is that the Kolmogorov flow studied here is analogous to realistic shear flows, such as those through channels and over bounding surfaces (*i.e.*, in boundary layers). If, in such cases, the flow also shows spectral anisotropy (and increasingly so) at higher and higher wave numbers, then this basic finding represents a new factor for incorporation into turbulence models. However, the assumption of the isotropy of those physical quantities which are primarily determined by the large scales of the turbulent motion is not invalidated as a useful approximation by the present results.

Acknowledgements. We would like to thank G. Erlebacher, S. Girimaji, and Y. Zhou of ICASE and B. Younis of City University, London, for their useful comments.

References

[1] O. Reynolds, "An experimental investigation of the circumstances which determine whether the motion of water shall be direct or sinuous, and of the law of resistance in parallel channels," Phil. Trans. Roy. Soc. Lond. **Part III**, 935 (1883).

[2] J. Laufer, "The structure of turbulence in fully developed pipe flow," NACA Rep. 1174 (1954).

[3] A. K. M. F. Hussain & W. C. Reynolds, "Measurements in fully developed turbulent channel flow," J. Fluids Eng. **97**, 568 (1975).

[4] H.-P. Kreplin & H. Eckelmann, "Behavior of the three fluctuating velocity components in the wall region of a turbulent channel flow," Phys. Fluids **22**, 1233 (1979).

[5] P. S. Klebanoff, "Characteristics of turbulence in a boundary layer," NACA Rep. 1247 (1955).

[6] L. P. Purtell & P. S. Klebanoff, "Turbulent boundary layer at low Reynolds number," Phys. Fluids **24**, 802 (1981).

[7] F. H. Champagne, V. G. Harris, & S. Corrsin, "Experiments on nearly homogeneous turbulent shear flow," J. Fluid Mech. **41**, 81 (1970).

[8] V. G. Harris, J. A. Graham, & S. Corrsin, "Further experiments on nearly homogeneous turbulent shear flow," J. Fluid Mech. **81**, 657 (1977).

[9] S. & S. Corrsin, "Experiments in nearly homogeneous turbulent shear flow with a uniform temperature gradient. Part 1," J. Fluid Mech. **104**, 311 (1981).

[10] S. Tavoularis & U. Karnik, "Further experiments on the evolution of turbulent stresses and scales in uniformly sheared turbulence," J. Fluid Mech. **204**, 457 (1989).

[11] D. C. Leslie, "Analysis of a strongly sheared, nearly homogeneous turbulent shear flow," J. Fluid Mech. **98**, 435 (1980).

[12] R. S. Rogallo, "An ILLIAC program for the numerical simulation of homogeneous incompressible turbulence," NASA TM-73203 (1977).

[13] W. J. Feiereisen, W. C. Reynolds, & J. H. Ferziger, "Numerical simulation of a compressible, homogeneous, turbulent shear flow," Report No. TF-13, Stanford Univ., California (1981).

[14] R. S. Rogallo, "Numerical experiments in homogeneous turbulence," NASA TM-81315 (1981).

[15] S. Sarkar, G. Erlebacher, & M. Y. Hussaini, "Direct simulation of compressible turbulence in a shear flow," Theoret. Comput. Fluid Dynamics **2**, 319 (1991).

[16] G. Sivashinsky & V. Yakhot, "Negative viscosity effect in large-scale flows," Phys. Fluids **28**, 1040 (1985).

[17] G. Sivashinsky, "Weak turbulence in periodic flows," Physica D **17**, 243 (1985).

[18] Z. S. She, "Metastability and vortex pairing in the Kolmogorov flow," Phys. Lett. A **124**, 161 (1987).

[19] Z. S. She, "Large-scale dynamics and transition to turbulence," in *Current Trends in Turbulence Research*, edited by H. Branover, M. Mond, & Y. Unger (AIAA, Washington D. C., 1988).

[20] A. L. Frenkel, "Stability of an oscillating Kolmogorov flow," Phys. Fluids A **3**, 1718 (1991).

[21] A. Thèss, "Instabilities in two-dimensional spatially periodic flows. Part 1: Kolmogorov flow," Phys. Fluids A **4**, 1718 (1992).

[22] D. Armbruster, R. Heiland, E. J. Kostelich, & B. Nicolaenko, "Phase space analysis of bursting behavior in Kolmogorov flow," Physica D **58**, 392 (1992).

[23] V. Borue & S. A. Orszag, "Numerical study of three-dimensional Kolmogorov flow at high Reynolds numbers," J. Fluid Mech. **306**, 293 (1996).

[24] P. G. Drazin & W. H. Reid, *Hydrodynamic Stability*, (Cambridge U. P., Cambridge, England, 1981), pp. 153-64.

[25] L. D. Landau & E. M. Lifshitz, *Fluid Mechanics*, 2nd Ed. (Pergamon, New York, 1987), pp. 95-8.

[26] E. Ott, *Chaos in Dynamical Systems* (Cambridge U. P., Cambridge, England, 1993), Chp. 3.

[27] J. Gazdag, "Time-differencing schemes and transform methods," J. Comp. Phys. **20**, 196 (1976).

[28] G. S. Patterson, Jr., & S. A. Orszag, "Spectral calculations of isotropic turbulence: Efficient removal of aliasing interaction," Phys. Fluids **14**, 2538 (1971).

[29] G. K. Batchelor, *The Theory of Homogeneous Turbulence* (Cambridge U. P., Cambridge, England, 1953), Chp. VI.

[30] C. G. Speziale & P. A. Durbin, "Local anisotropy in strained turbulence at high Reynolds numbers," J. Fluids Engineering **113**, 707 (1991).

[31] C. J. Lawn, "The determination of the rate of dissipation in turbulent pipe flow," J. Fluid Mech. **48**, 477 (1970).

[32] W. D. McComb, *The Physics of Fluids Turbulence* (Clarendon Press, Oxford, England, 1990), p. 82.

[33] B. E. Launder, G. J. Reece, & W. Rodi, "Progress in the development of a Reynolds-stress closure," J. Fluid Mech. **68**, 537 (1975).

[34] C. W. Van Atta & W. Y. Chen, "Measurements of spectral energy transfer in grid turbulence," J. Fluid Mech. **38**, 743 (1969).

Table 1. Comparison with Experimental Results.

Source	$-Q_{zx}$	B_x	B_y	B_z
Linear shear ([33], Table 1)	0.48	0.30	-0.12	-0.18
Near-wall turb. ([33], Table 1)	0.45	0.51	-0.09	-0.42
Linear shear ([9], Table 4)	0.45	0.39	-0.10	-0.29
Sinusoidal shear (this paper)	0.45	0.08	-0.07	-0.01

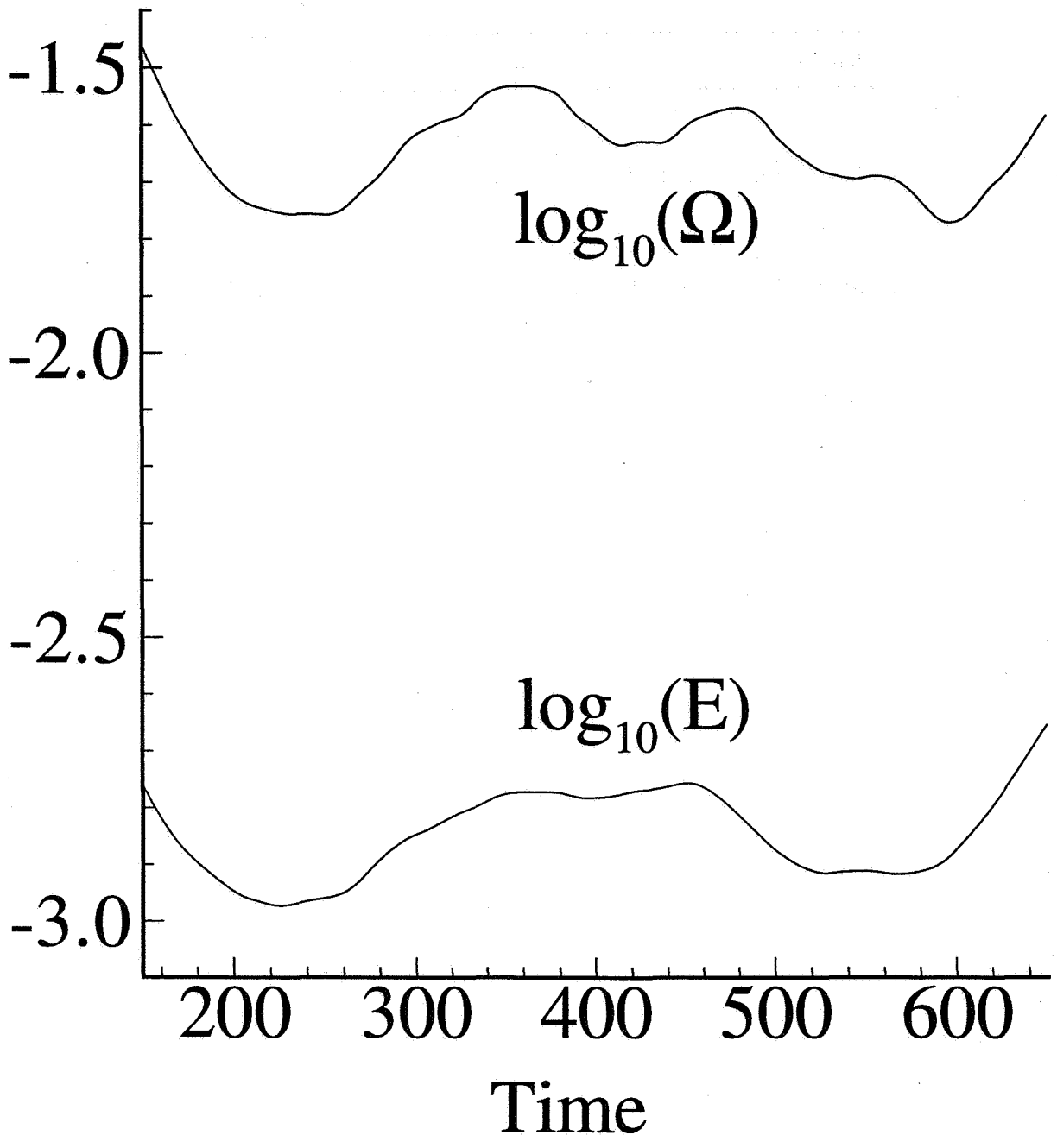

Figure 1. Turbulent energy E and enstrophy Ω versus time.

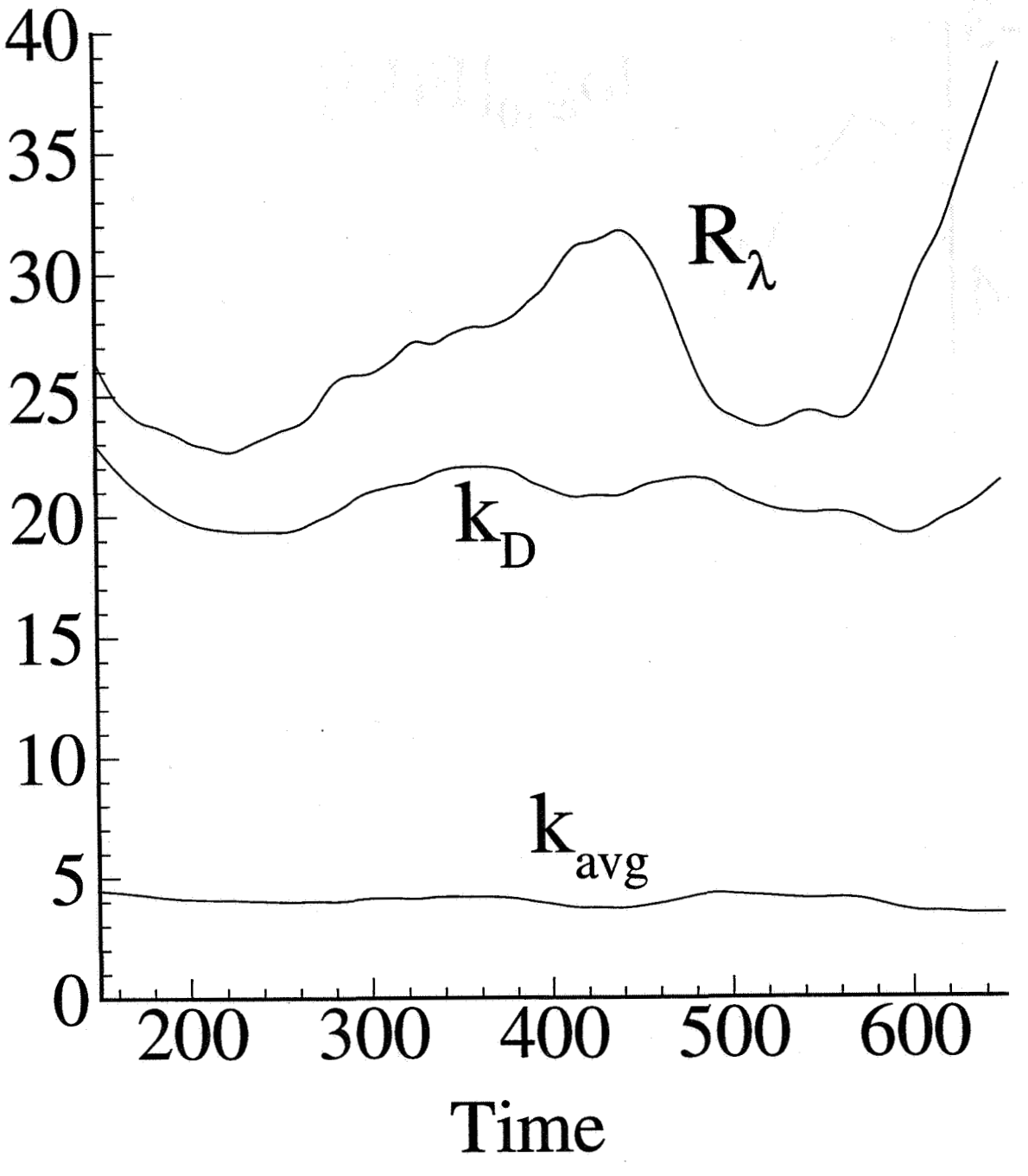

Figure 2. Average wave number k_{avg}, dissipation wave number k_D, and microscale Reynolds number R_λ versus time.

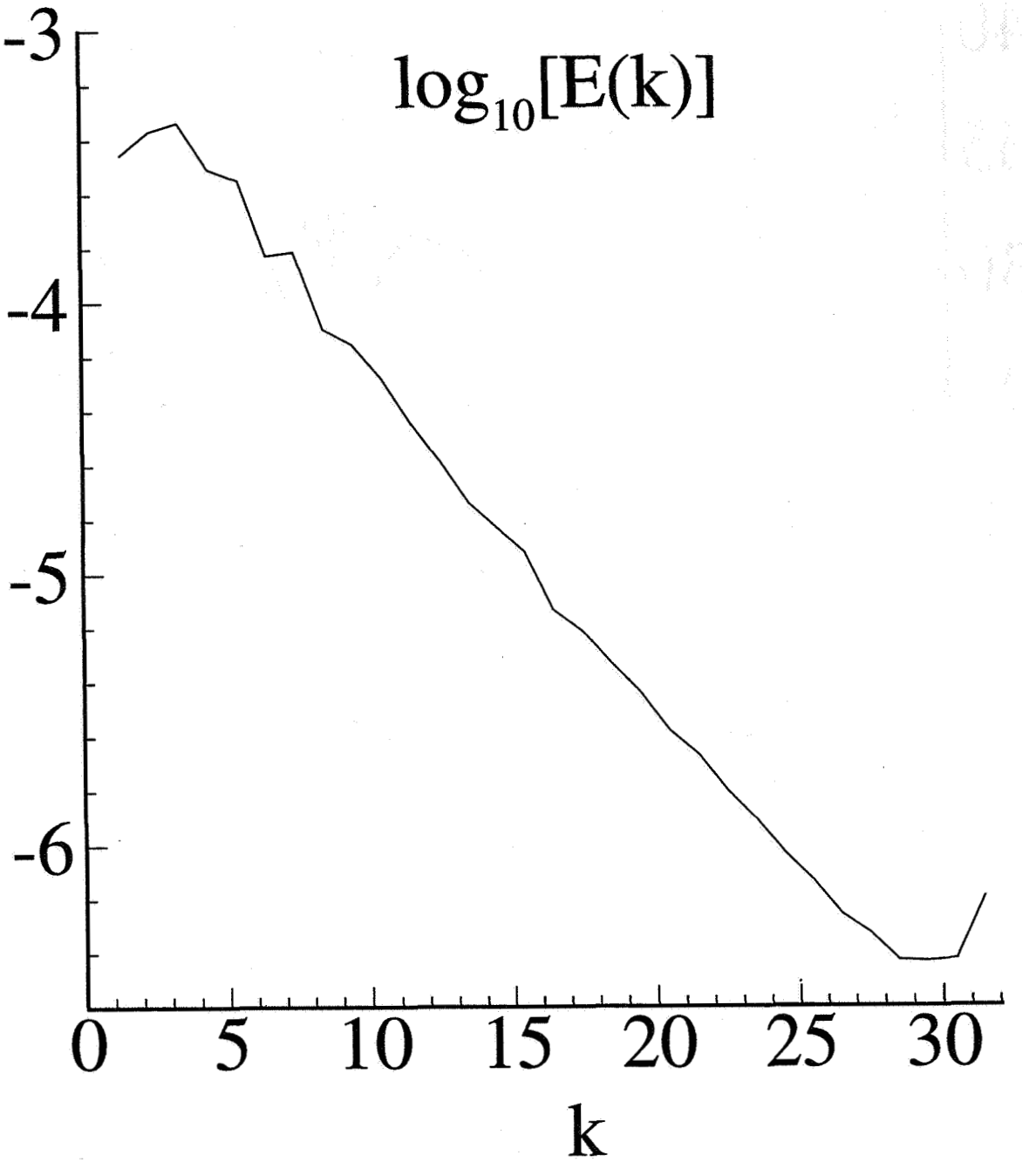

Figure 3. Averaged turbulent energy spectrum $E(k)$ versus wave number magnitude k.

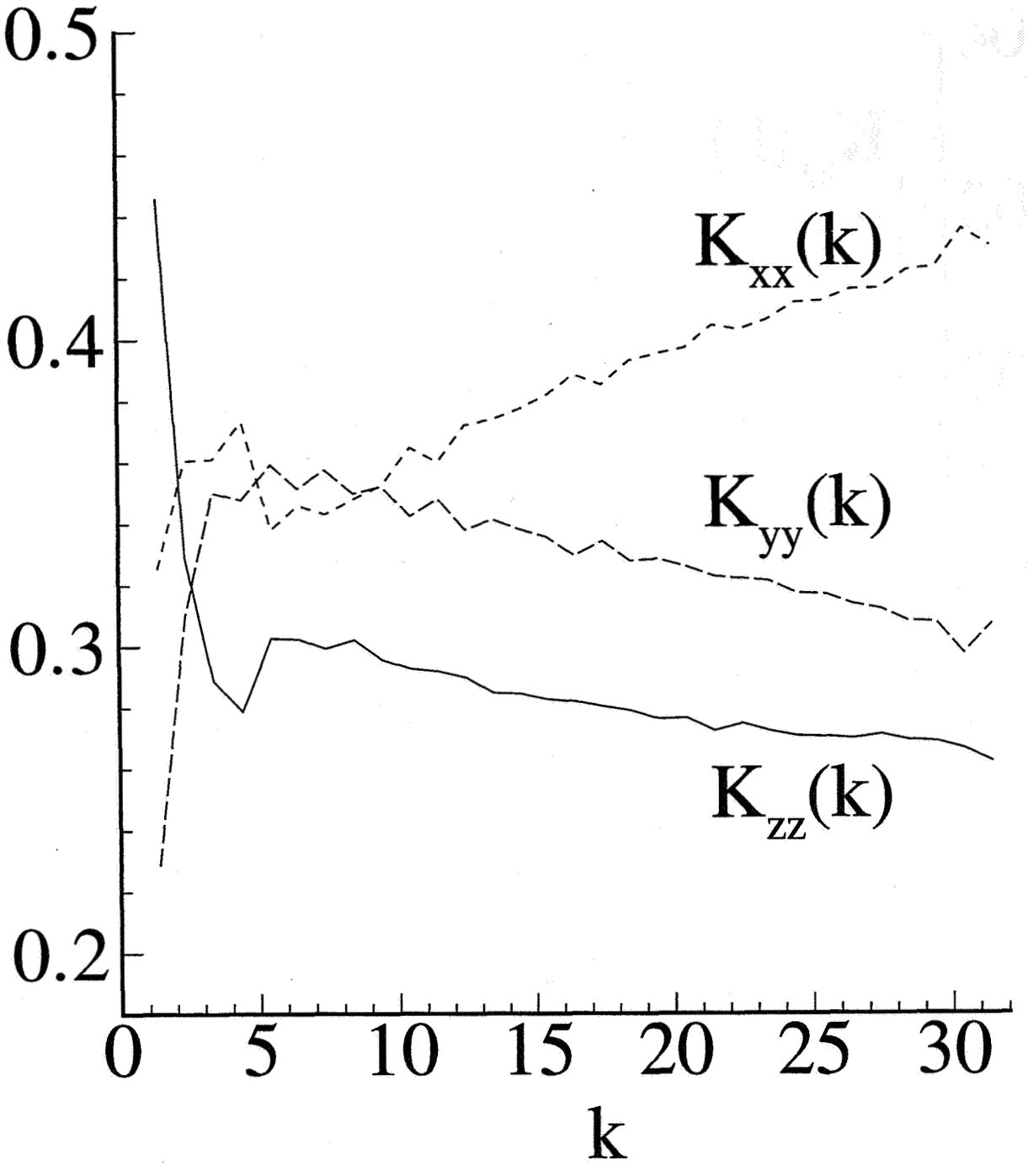

Figure 4. Averaged diagonal Kolmogorov anisotropy components versus wave number magnitude.

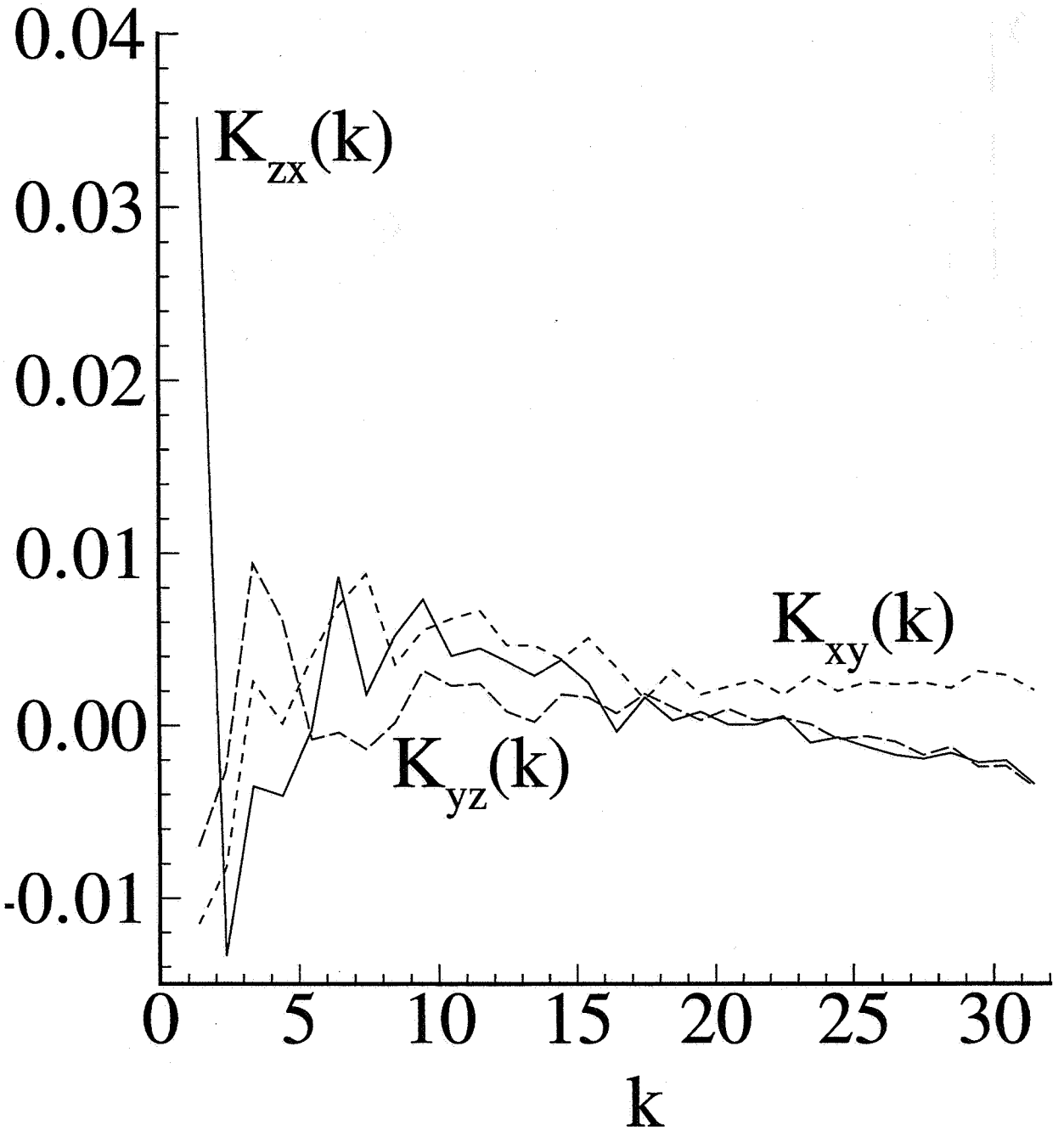

Figure 5. Averaged off-diagonal Kolmogorov anisotropy components versus wave number magnitude.

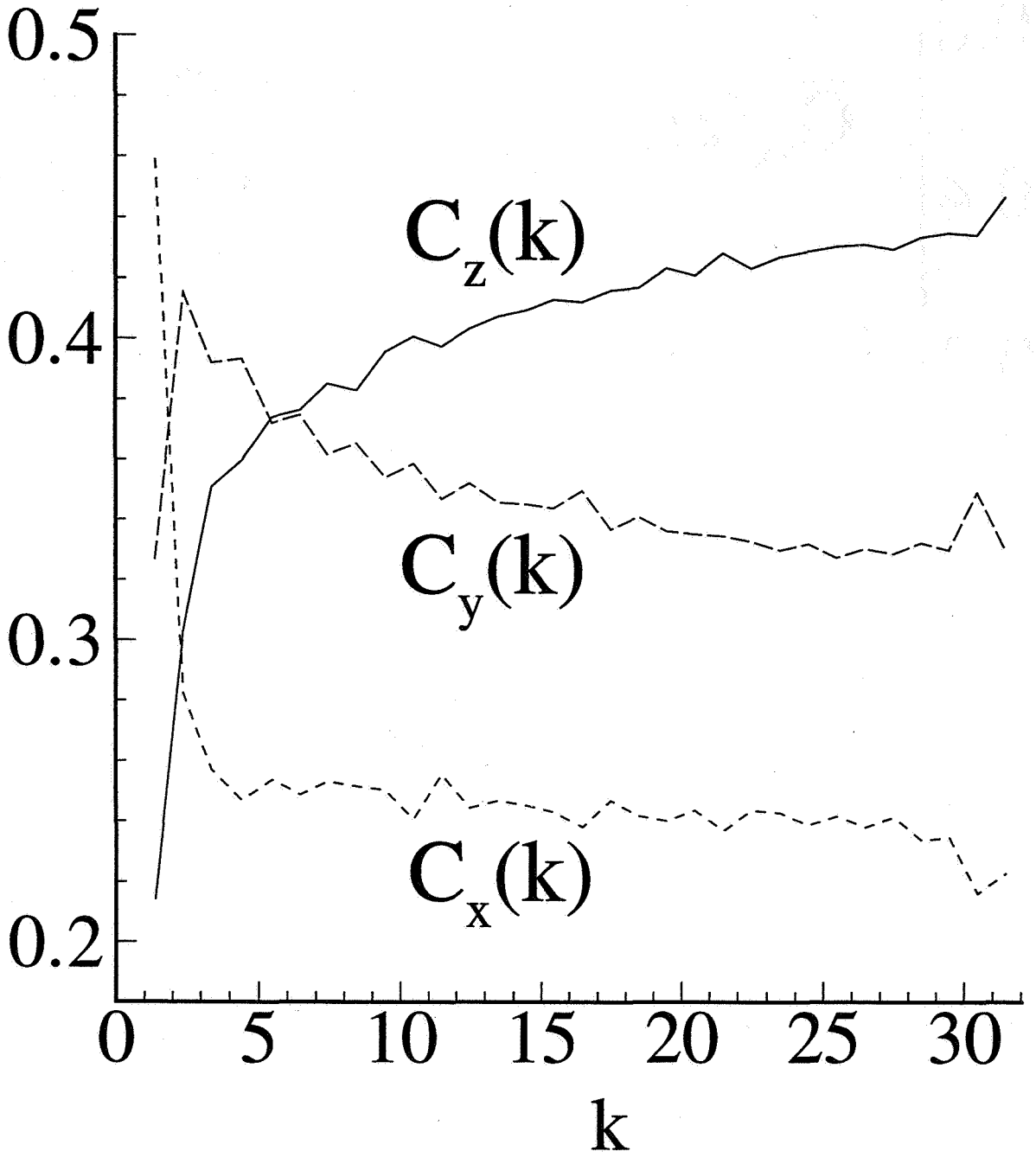

Figure 6. Averaged k^2-anisotropy coefficients versus wave number magnitude.

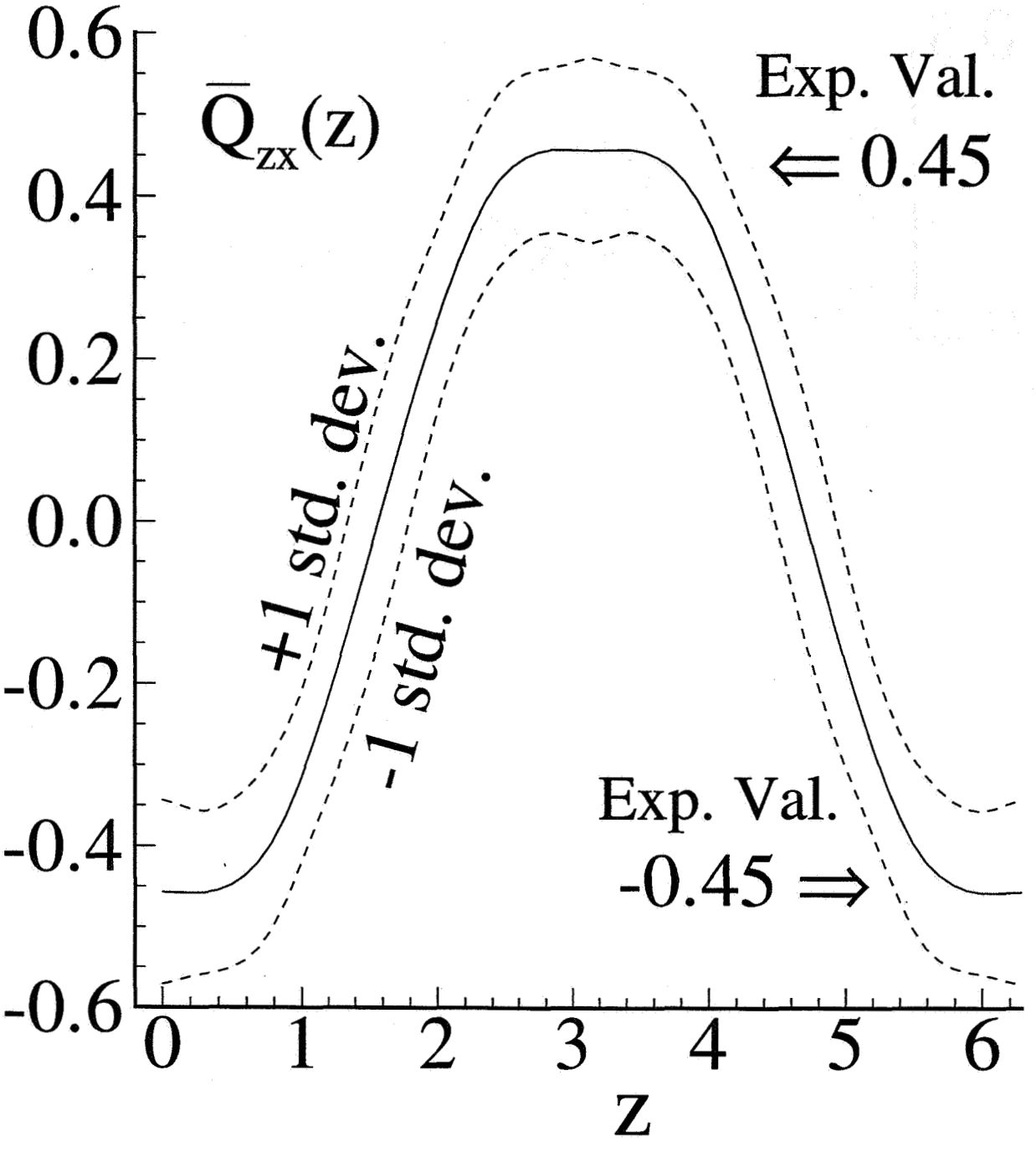

Figure 7. Averaged cross-correlation $\bar{Q}_{zx}(z)$ versus z.

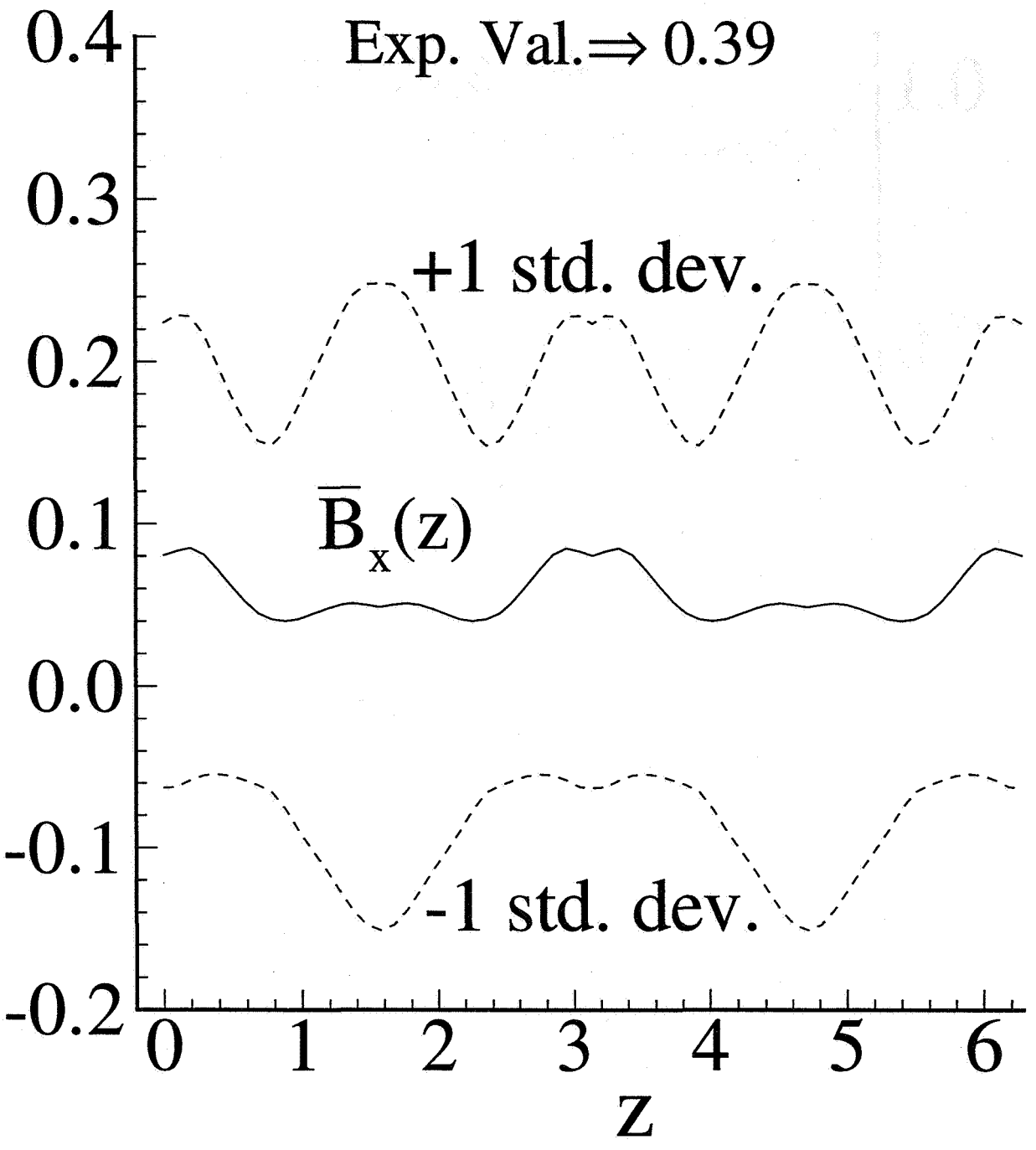

Figure 8. Averaged stress anisotropy component $\bar{B}_x(z)$ versus z.

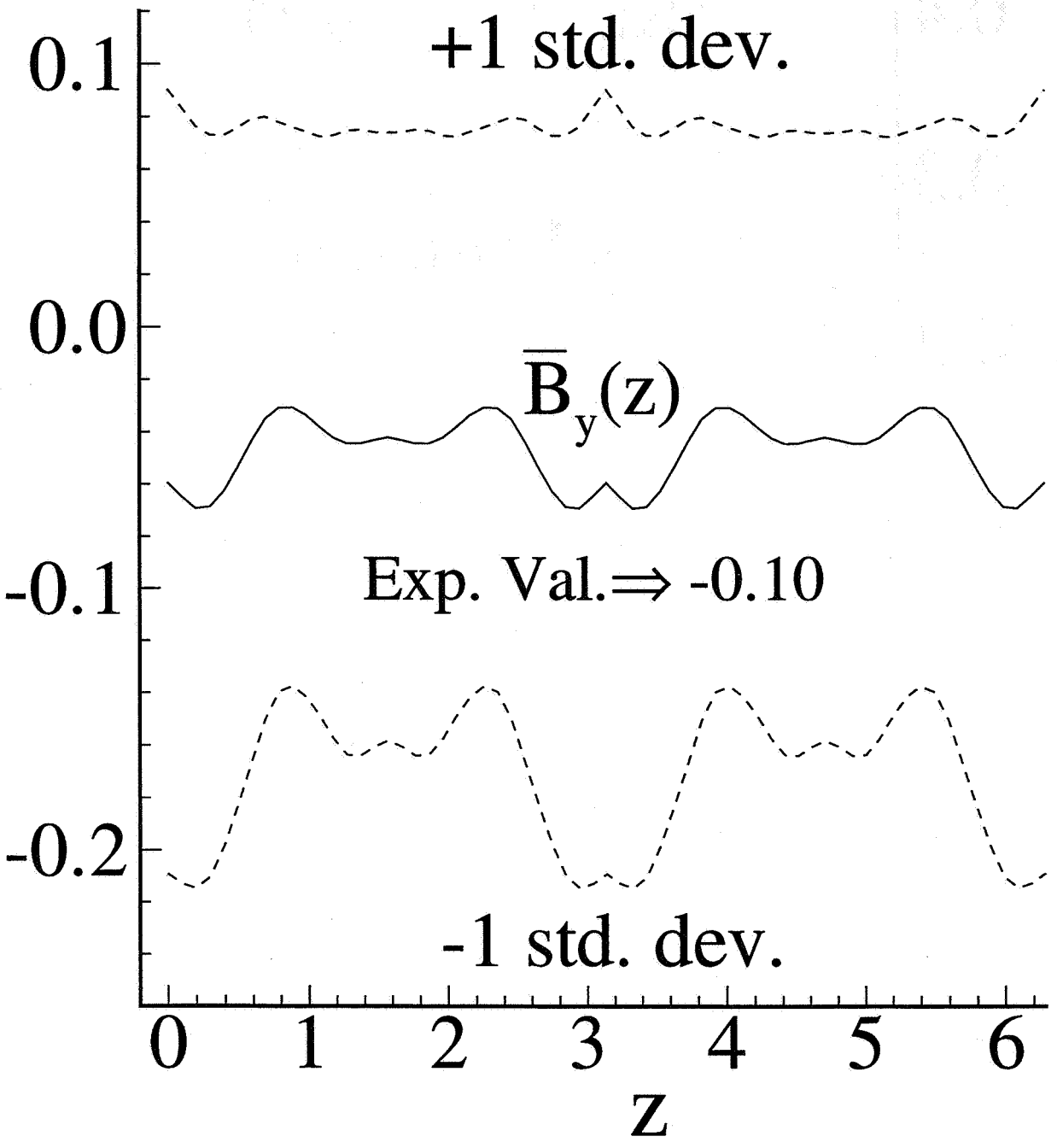

Figure 9. Averaged stress anisotropy component $\bar{B}_y(z)$ versus z.

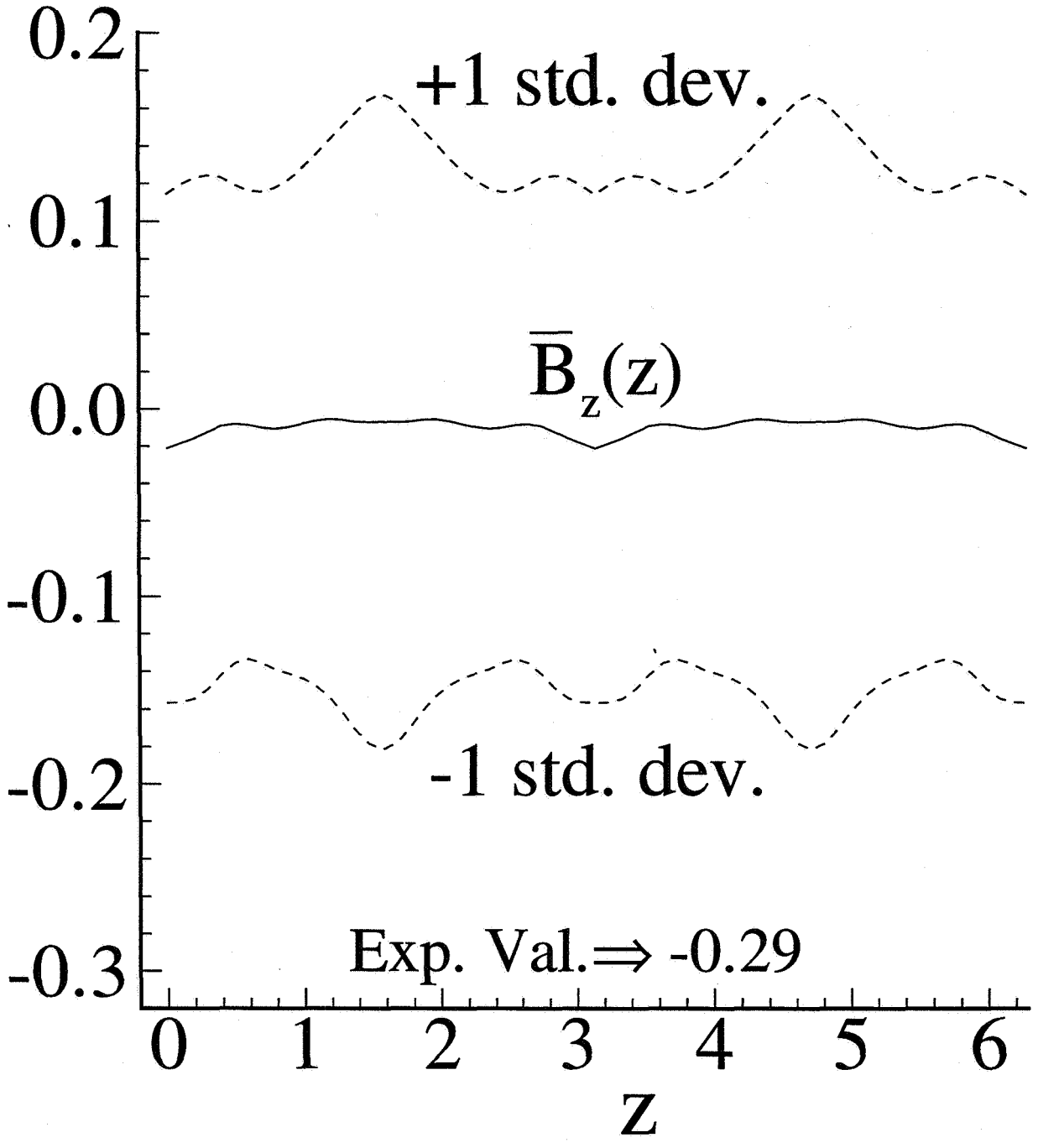

Figure 10. Averaged stress anisotropy component $\bar{B}_z(z)$ versus z.

REPORT DOCUMENTATION PAGE

Form Approved
OMB No. 0704-0188

1. AGENCY USE ONLY *(Leave blank)*

2. REPORT DATE
March 1996

3. REPORT TYPE AND DATES COVERED
Contractor Report

4. TITLE AND SUBTITLE
KOLMOGOROV FLOW IN THREE DIMENSIONS

5. FUNDING NUMBERS
C NAS1-19480
WU 505-90-52-01

6. AUTHOR(S)
John V. Shebalin
Stephen L. Woodruff

7. PERFORMING ORGANIZATION NAME(S) AND ADDRESS(ES)
Institute for Computer Applications in Science and Engineering
Mail Stop 132C, NASA Langley Research Center
Hampton, VA 23681-0001

8. PERFORMING ORGANIZATION REPORT NUMBER
ICASE Report No. 96-24

9. SPONSORING/MONITORING AGENCY NAME(S) AND ADDRESS(ES)
National Aeronautics and Space Administration
Langley Research Center
Hampton, VA 23681-0001

10. SPONSORING/MONITORING AGENCY REPORT NUMBER
NASA CR-198319
ICASE Report No. 96-24

11. SUPPLEMENTARY NOTES
Langley Technical Monitor: Dennis M. Bushnell
Final Report
To be submitted to Physics of Fluids.

12a. DISTRIBUTION/AVAILABILITY STATEMENT
Unclassified–Unlimited

Subject Category 34

12b. DISTRIBUTION CODE

13. ABSTRACT *(Maximum 200 words)*

A numerical study of the long-time evolution of incompressible Navier-Stokes turbulence forced at a single long-wavelength Fourier mode, *i.e.*, a Kolmogorov flow, has been completed. The boundary conditions are periodic in three dimensions and the forcing is effected by imposing a steady, two-dimensional, sinusoidal shear velocity which is directed along the x-direction and varies along the z-direction. A comparison with experimental data shows agreement with measured cross-correlations of the turbulent velocity components which lie in the mean-flow plane. A statistical analysis reveals that the shear-driven turbulence studied here has significant spectral anisotropy which increases with wave number.

14. SUBJECT TERMS
Kolmogorov flow; turbulence; direct numerical simulation

15. NUMBER OF PAGES
25

16. PRICE CODE
A03

17. SECURITY CLASSIFICATION OF REPORT	18. SECURITY CLASSIFICATION OF THIS PAGE	19. SECURITY CLASSIFICATION OF ABSTRACT	20. LIMITATION OF ABSTRACT
Unclassified	Unclassified		